Journal of Arid Environments 193 (2021) 104587

Contents lists available at ScienceDirect

Journal of Arid Environments

journal homepage: www.elsevier.com/locate/jaridenv

Evaluating post-fire recovery of Latroon dry forest using Landsat ETM+, unmanned aerial vehicle and field survey data

Bassam Qarallah [a], Malik Al-Ajlouni [a], Ayman Al-Awasi [b], Mohammad Alkarmy [b], Emad Al-Qudah [c], Ahmad Bani Naser [b], Amani Al-Assaf [d], Caroline M. Gevaert [e], Yolla Al Asmar [e], Mariana Belgiu [e], Yahia A. Othman [a,*]

[a] Department of Horticulture and Crop Science, The University of Jordan, Amman, 11942, Jordan
[b] Department of Forestry, Ministry of Agriculture, Jerash, Jordan
[c] Land and Irrigation Department, Ministry of Agriculture, Amman, Jordan
[d] Department of Agricultural Economics and Agribusiness, The University of Jordan, 11942, Jordan
[e] Faculty of Geo-Information Science and Earth Observation, University of Twente, 7522, NB Enschede, the Netherlands

ARTICLE INFO

Keywords:
Remote sensing
Forest fires
dNBR
Drones
UAV
Pinus

ABSTRACT

We evaluated the fire severity and recovery process of the Latroon dry forest in Jordan following the 2003 fire. A series of multi-temporal Landsat-ETM + data and the delta normalized burn ratio (dNBR) were used to map the fire severity immediately following the fire and 1,5,9,13 and 17 years after. In addition, combined field morpho-physiological measurements, unmanned aerial vehicle (UAV) were also used in 2020 to assess the forest recovery. Landsat-dNBR images revealed that about 65% of the forest was burned in 2003. In 2020, about 90% of the burned area recovered to condition before fire. UAV means were similar to ground measurement data across the severity classes and over the tested species. Landsat-dNBR images showed that most moderate and highly severe burned area in 2003 had recovered in 2020 but ground measurements showed that the severely burned area trees were significantly shorter ($p < 0.001$) than those from the moderate severity across the studied species. Therefore, Landsat-dNBR did not detect tree height changes. While UAV can potentially estimate the tree height, Landsat-ETM+ (near-infrared, chlorophyll; shortwave-infrared, water status) hold promise for estimating the physiology of the canopy. Overall, different remote sensing levels are required to track different kinds of changes in the recovered forests.

1. Introduction

Forest fires are a significant disturbance variable in terrestrial ecosystems on a global scale and contribute extensively to the budgets of several greenhouse gases including CO_2 and CH_4 (Langenfelds et al., 2002; Van Der Werf et al., 2010). Severe wildfires negatively impact water, environmental resources and human life, specifically socio-economic factors (Quintano et al., 2019). In addition, forest fires may cause: irreparable damage to the environment and atmosphere, long-term negative impact on global warming, and extinction of rare species of the flora and fauna (Alkhatib, 2014). Fire severity depends on vegetation health (e.g. leaf moisture content, transpiration and chlorophyll content), community composition, climate, weather conditions and topography (Cansler and McKenzie, 2014; Gibson et al., 2020; Hammill and Bradstock, 2006; Keeley and Syphard, 2016). Climate change is expected to intensify fire impacts on natural ecosystems (Keeley and Syphard, 2016). Therefore, monitoring and predicting fire activities is prerequisite to understand our changing climate, specifically global warming (Van Der Werf et al., 2010; Wei et al., 2020). In addition, modeling forest fires can reduce the response time, the potential damage and the cost of firefighting (Alkhatib, 2014).

Fire mapping provide authorities a temporal and spatial overview of fire severity in order to orient management and future planning. It also plays a key role in advancing climate change and ecological studies (Flannigan et al., 2009; Gibson et al., 2020). Modeling forest fires requires historical and spatial scale analyses that associate annual fires to climate variation, understanding of how temperature and rainfall interact to control fire severity, and fuel structure (Keeley and Syphard, 2016). However, traditional monitoring and modeling of forest fires requires intensive human and material resources and might be

* Corresponding author. Department of Horticulture and Crop Science, The University of Jordan, Amman, 1194, Jordan.
E-mail address: ya.othman@ju.edu.jo (Y.A. Othman).

https://doi.org/10.1016/j.jaridenv.2021.104587
Received 9 May 2021; Received in revised form 2 June 2021; Accepted 30 June 2021
Available online 5 July 2021

inaccurate. Interestingly, remote sensing can upscale the spatial analysis and potentially capture accurate relationships between climate and fires (Keeley and Syphard, 2016). Advanced sensing technologies such as remote sensing are increasingly used for fire monitoring recently because it provides an overview of long-term spatio-temporal overview of active fires over long period (Wei et al., 2020). In addition, remotely-sensed data can upscale plant physiological responses to large area (Othman et al., 2014, 2021). In fact, the newer generation of remote sensing platforms (e.g. unmanned aerial vehicle, UAV) are now offering high spatial/temporal resolution, many opportunities for fine-scale ecological mapping and are capable of capturing new imagery at daily return intervals (Arnett et al., 2015). In south-eastern Australia, the combined used of Sentinel-2 images and a random forest model successfully mapped fire severity (Gibson et al., 2020). The accuracy percentage for the unburnt and extreme severity class was higher than 95%, while the low and moderate severity classes ranged from 70% to 85%. Trees moisture content is one of the essential factors affecting ignition and spread of wildfire. Trees sap (water) has strong absorption features in the shortwave infrared (SWIR) spectrum, which provide a sensing basis for direct estimation of live fuel moisture content (Yebra et al., 2013).

Accurate burn severity estimates are critical for post-fire management. The burn severity variable integrates both direct fire effects (vegetation depletion) and ecosystem responses (vegetation regeneration) (Veraverbeke et al., 2011). Multispectral remote sensing data such as spectral indices-based are becoming essential for burned area and burn severity mapping because they provide accurate and consistent information about the fire activity, extent and severity (Chuvieco et al., 2002; Quintano et al., 2019; Veraverbeke et al., 2011). In this context, most work on post-fire losses are derived from Landsat and Sentinel-2 surface reflectance data, mainly because of their adequate spatial and temporal resolutions (Filipponi, 2019; French et al., 2008). The normalized burn ratio (NBR) has been linked to vegetation moisture content by combining the near infrared (NIR) and SWIR wavelengths. Shortwave infrared spectrum regions are associated with water status of plants (Othman et al., 2014, 2015). In addition, the difference between pre- and post-fire images (delta NBR, dNBR) has been recognized as a standard method to estimate the burn severity from remotely-sensed data (Quintano et al., 2019; Veraverbeke et al., 2011). The dNBR consider the short-term impact (preliminary assessment) of fire from an immediate post-fire NBR (difference between pre-fire NBR and the immediate post-fire NBR) and the long-term impact (extended assessment) from post-fire NBR image a year or more after a fire (Quintano et al., 2019). In sum, the dNBR can provide bi-temporally differenced information about the burn severity which has proven to be valuable for obtaining detailed information over specific fires (Veraverbeke et al., 2011).

Jordan has long, dry, hot summers, and relatively short cold winters. Forests in Jordan cover 800 km^2 or less than 1% of the total area of Jordan. The Jerash and Ajloune forests account for more than 50% of these forests. This area hosts about 190 km^2 of the southernmost native *Pinus halepensis* forest in the world and the last remaining stand of old pine forest in Jordan (Al-Eisawi, 2012). Even in such fragmented and small pine forest areas, rural communities still appreciate forest ecosystems. Previous research elucidated the social-ecological system of forests in Jordan (Shishany et al., 2020, Al-assaf et al., 2014). These studies emphasized the social dimension that reflects the relation between the forest and people, where forests are recognized for their financial contribution by providing provisioning services (i.e wood, and non-wood products as grazing, medicinal and edible plants), and cultural services (i.e. recreation, tourism) (Al-Assaf et al., 2016; Al-assaf et al., 2014). Shishany et al. (2020) highlighted the relational values of forest and people in Jordan, and how people are an important component in forest management plans, which depend on their raised awareness of the sustainable forest ecosystem.

Forest fires due to hot dry climate and illegal logging are the main threats to Jordanian forests. In 2019, more than 200 fires were reported by the Forestry Department in Jordan. In addition, authorities encounter huge challenges to mitigate the impact of forest fires and orient their efforts due to the difficulties of accurately estimating the actual area exposed to fire directly after the fire incidence as well as the recovery rate of burned spots. Satellite images are an ideal dataset to examine the extent and impact of forest fires (Arnett et al., 2015). Vegetation indices derived using surface reflectance images are widely used because those indices normalize the magnitude of change between the multi-temporal images (adjust the variation in spectral levels) and are associated with the variation in structural and physiological plant processes including gas exchange, chlorophyll, leaf area and water status (Gao, 1996; Huete et al., 2002; Othman et al., 2014, 2015, 2019, 2021; Tadros et al., 2020). However, for successful mapping of fire/burn severity, recovery status and consequently forest health, combined field sampling and satellite surface reflectance data of burn condition is essential (French et al., 2008). On August 28, 2003, the Latroon Mountain forests, Jerash, Jordan experienced a severe fire which damaged most trees on this mountain. The regeneration is still under progress. However, no reliable data quantifying the total area, severity or recovery process of this burned area is currently available. We believe that remote sensing data from Landsat ETM+ (2003–2020) coupled with UAV and ground physiological measurements (2020) can provide an overview of forest fire severity in 2003, the recovery process as well as the forest status after 17 years of fire incidence. The objective of this study was to estimate the historical burn extent and severity in Latroon Mountain dry forest using Landsat-dNBR images between 2003 and 2020 as well as the regeneration percentage. In addition, the current forest status (2020) was evaluated using Landsat-dNBR images, UAV images and ground physiological measurements (gas exchange, canopy temperature and chlorophyll content index).

2. Materials and methods

2.1. Study area

The study was conducted at Jerash (Latroon Mountain), Jordan (32°17′32.71″ N, 35°49′09.87″E, elevation ranges from 1030 to 1130 m above sea level). Mean annual precipitation ranged from 250 to 400 mm. The mean annual maximum temperature ranges from 20 to 28 °C and the minimum temperature ranges from 10 to 15 °C. The study area covers an area of 30 ha (Fig. 1). The main vegetation species *Arbutus andrachne*, *Quercus coccifera*, and *Pinus halepensis*. In the summer of 2003 (August 28, 2003), several large wildfires of unknown cause struck Jordanian forests. The fires were the worst natural disaster of the last decades in Jeresh, specifically the Latroon Mountain. The fires consumed more than 60% of the vegetation.

2.2. Image acquisition, pre-processing, and classification

Surface reflectance data from Landsat ETM+ was used to detect vegetation cover change before fire incidence on August 28, 2003 and the regeneration process thereafter, from October 2003 to August 2020. ETM + images dates were: one month before the fire (July 2003), one month after fire (October 2003), one (August 2004), five (August 2008), nine (August 2012), thirteen (August 2016) and seventeen (August 2020) years after the forest fire. We selected the August time to ensure that only shrubs and trees are captured in the images. At springtime (March–April), the area is normally covered with grasses as well as shrubs and trees. These grasses die around June–July and after that only shrubs and trees are detected.

Cloud-free Landsat ETM + images were downloaded from the EarthExplorer website. Landsat ETM + collection 2, level 2 were used. Those images (surface reflectance climate data records) are atmospherically corrected, available for free, and they are a reliable source for change detection studies, especially for vegetation (Othman et al.,

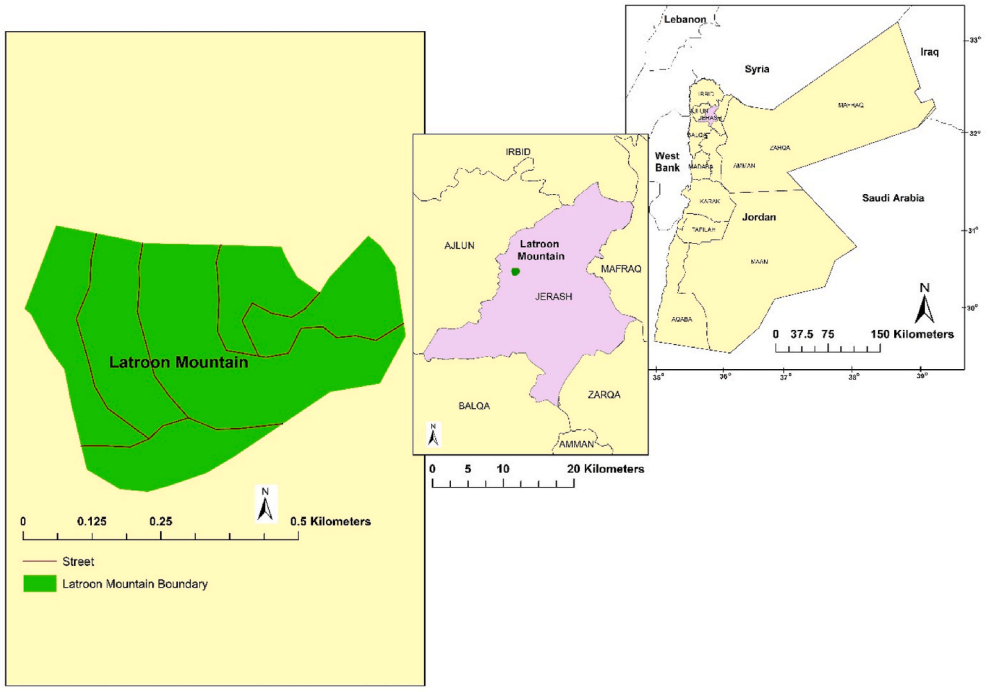

Fig. 1. Location of the Latroon Mountain study area in Jerash, Jordan.

2018; Sawalhah et al., 2018). Geo-referencing was conducted using Environment for Visualizing Images (ENVI) 5.0 (Research Systems, Boulder, Colorado, USA). In addition, radiometric correction was applied using the Fast Line-of-sight Atmospheric Analysis of Spectral Hypercubes (FLAASH) algorithm in ENVI to normalize the different Landsat datasets. In FLAASH, Rural Aerosol model was used and the visibility was set to 40 km. Burned area and the recovery spots were identified using NBR (Equation (1)).

$$NBR = \frac{(NIR - SWIR)}{(NIR + SWIR)} \quad (1)$$

Where NIR is band 4 in ETM+ and SWIR is band 7. The difference between the pre-fire and post-fire NBR obtained from the images is used to calculate the delta NBR (dNBR or ΔNBR), which then were used to estimate the burn severity. The dNBR classification scheme of Landsat ETM + datasets (UNOOSA, 2021) for the study area is found in Table 1.

2.3. Aerial imaging system

An Unmanned Aerial Vehicle (UAV) with a digital camera (Zen muse, Z30; Germany) on board was used to obtain post-fire surface reflectance images on the blue, green, red bands at high spatial resolution (10 cm) (Fig. 2). The flight was carried out in September 2020. A series of aerial images (~400 images) for the mountain were acquired and processed using Pix4D software. The products obtained from the Digital Surface Model (DSM), Digital Terrain Model (DTM) and orthorectified image.

Table 1
The dNBR classification scheme of Landsat ETM + datasets for the study area. Burn severity levels obtained by calculating delta Normalized Burn Ratio (dNBR), (UNOOSA, 2021).

dNBR range	Fire severity level
−0.5–0.1	Un-burned, enhanced regrowth
0.1–0.25	Low severity
0.25–0.45	Low to moderate severity
0.45–0.65	Moderate to severe
0.65–1.3	High severity

Fig. 2. Unmanned Aerial Vehicle (UAV) system, M210 V2 quad copter with a Zen muse digital camera onboard. The UAV camera acquire images on the blue, green, red bands at high spatial resolution (10 cm) at 70 m flight height. (For interpretation of the references to colour in this figure legend, the reader is referred to the Web version of this article.)

The images dataset was acquired with the quad copter UAV (M210 V2, Da-Jiang Innovations, China). The UAV flight height was 70 m and images were collected at a 70% overlap. For horizontal accuracy of the flight, six ground control points were determined and linked to image.

2.4. Tree physiological measurements

Tree height, gas exchange (photosynthesis *Pn*, stomatal conductance *gs*, and transpiration *E*), leaf and canopy temperatures and chlorophyll content index (SPAD) were determined during the summer time, July–August 2020. Physiological measurements were conducted between 10:00 a.m. and 1:00 p.m. and synchronized with the UAV and satellite

overpass date. All measurements were in moderate and high severity fire plots that occurred in 2003 and identified using the Landsat-dNBR images. Gas exchange measurements and leaf temperature were determined using a portable photosynthesis system (LI-6400XT; LI-COR, Lincoln, NE, USA) and following the procedures of Othman et al. (2014). Gas exchange measurements were from two sun-exposed and fully-mature leaves. Light intensity was set to track ambient photosynthetically active radiation, area of chamber head to 6 cm^2, flow rate to 500 µmol s^{-1}, temperature in the cuvette to ambient air and reference CO_2 to 400 µmol (Leskovar and Othman, 2021). The chlorophyll content index was determined using a chlorophyll meter (CCM-200 plus; Opti-Science, NH, USA) and canopy temperature measured using infrared thermometer (568, Fluke Corporation, Everett, WA, USA). The detector CCM-200 plus analyzes the ratio of two wavelengths to determine chlorophyll con-centration index. The index is not the content of chlorophyll *a*, *b* or total. Plant height for the three species were determined and compared to those derived using aerial images (DSM, DTM). Seven trees (per species) from the moderate-severe and high severity classes (42 trees in total) were selected for measurements. The selected trees were from the pixels classified as moderate-severe or highly severe in the 2003 dNBR image and low severity in the 2020 dNBR image. Our objective was to assess if the different severity classes identified in the 2020 dNBR image showed the same patterns as the UAV data and field measurements.

2.5. Graphing and statistical analysis

The analysis of variance (ANOVA) and the Tukey's HSD test ($P \leq 0.05$) in SAS (Version 9.4 for Windows; SAS Institute, Cary, NC) were used to identify differences between dNBR levels for physiological measurements. ArcMap (Version 10.2 for Windows; ESRI, Redlands, CA) was used to generate the study maps and to calculate the total burned area. Sigmaplot (Version 10.0 for Windows; Systat Software, San Jose, CA) was used to graph the ground measurement results, 2020.

3. Results

3.1. Assessment of forest fire severity and recovery using landsat ETM + data

Landsat-dNBR images revealed that the total area of moderate and high severity dNBR classes were zero in July 2003, one month before fire (Fig. 3, Table 2). The dNBR image in July 2003 was derived using two NBR-Landsat images captured immediately before fire. Because the vegetation changes in the area within the month (prior to fire) was limited, the NBR values for both images were approximately similar and therefore the dNBR was close to zero. One month after fire (October 2003), Landsat-dNBR images revealed that about 65% of the Latroon Mountain was burned. About 8% of the forest was severely burned (dNBR, 0.65–1.3), 14.8% moderate to severe (dNBR, 0.45–0.65), 19.5% low to moderate and 22.4 of the forest area were within the low severity fire dNBR class (Table 2). The 2020 Landsat-dNBR image revealed that the forest had potentially recovered (Fig. 3). The moderate and severe class areas (dNBR, 0.25–1.3) disappeared. However, at that date (17 years after the fire), about 9% of those burned lands were within the low severity class (dNBR, 0.1–0.25).

3.2. Tree morphology and physiological assessment

The current status of the forest was assessed through the tree morphology (plant height) and physiology (*Pn*, *E*, *gs*, leaf and canopy temperatures, and chlorophyll content index) in September 2020. In the burned area, the same tree and shrub species were found after 17 years of fire (2020). The dominate tree species in Latroon mountain in 2020 were *Arbutus andrachne*, *Pinus halepensis* and *Quercus coccifera* while *Cistus incanus* was the main shrub.

Tree height from ground measurements were compared to those from the UAV data. The morpho-physiological results were also linked to Landsat-dNBR results. Plant height was estimated by overlaying the DSM and DTM obtained with the UAV over the burned area (moderate and high severity classes, dNBR, 2003 image) (Fig. 4). Tree heights from the burned area were compared to ground measurements (Fig. 4). The

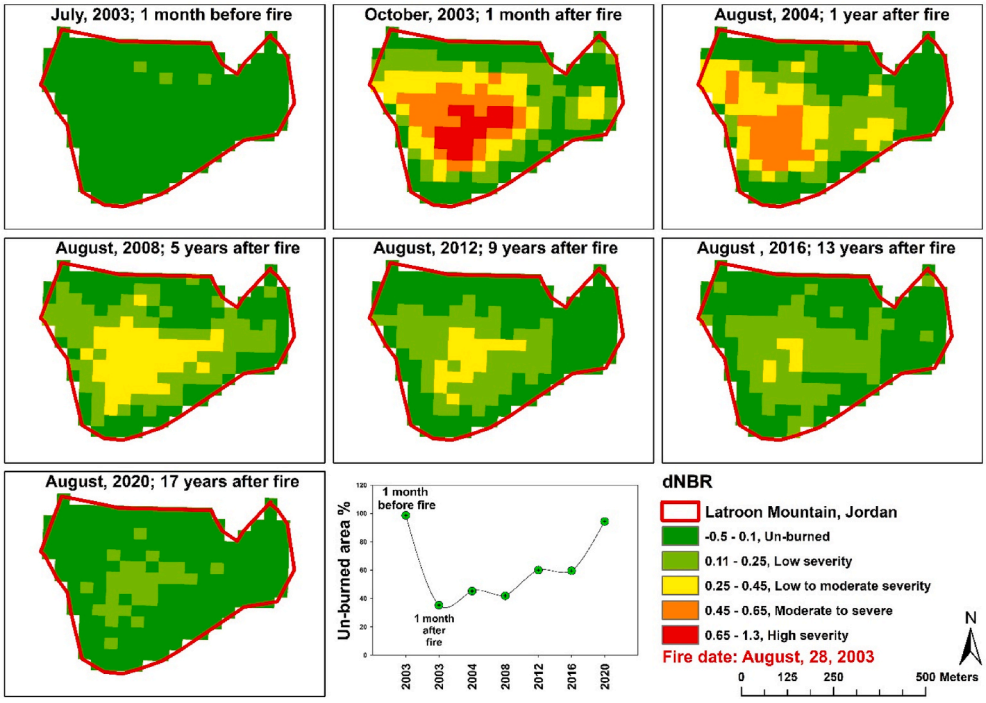

Fig. 3. Fire severity classes for Latroon Mountain before and after the forest fires classified from Delta Normalized Burn Ratio (dNBR) images derived from Landsat ETM + imagery.

Table 2
Burn severity classes for Latroon Mountain before and after the forest fires classified from Delta Normalized Burn Ratio (dNBR) images derived from Landsat ETM + imagery.

		Un-burned	Low severity	Low to moderate severity	Moderate to severe	High severity
Year	Coverage	(0.0–0.1)	(0.1–0.25)	(0.25–0.45)	(0.45–0.65)	(0.65–1.3)
2003 (1 month before fire)	Area (ha)	18.7	0.3	0.0	0.0	0.0
	%	**98.6**	**1.4**	**0.0**	**0.0**	**0.0**
2003 (1 month after fire)	Area (ha)	6.7	4.2	3.7	2.8	1.5
	%	**35.2**	**22.4**	**19.5**	**14.8**	**8.1**
2004 (1 year after fire)	Area (ha)	8.5	4.1	4.1	2.3	0.0
	%	**45.2**	**21.4**	**21.4**	**11.9**	**0.0**
2008 (5 years after fire	Area (ha)	7.9	6.8	4.2	0.0	0.0
	%	**41.9**	**35.7**	**22.4**	**0.0**	**0.0**
2012 (9 years after fire)	Area (ha)	11.4	5.9	1.7	0.0	0.0
	%	**60.0**	**31.0**	**9.0**	**0.0**	**0.0**
2016 (13 years after fire)	Area (ha)	11.3	7.1	0.5	0.0	0.0
	%	**59.5**	**37.6**	**2.9**	**0.0**	**0.0**
2020 (17 years after fire)	Area (ha)	17.8	1.1	0.0	0.0	0.0
	%	**94.3**	**5.7**	**0.0**	**0.0**	**0.0**

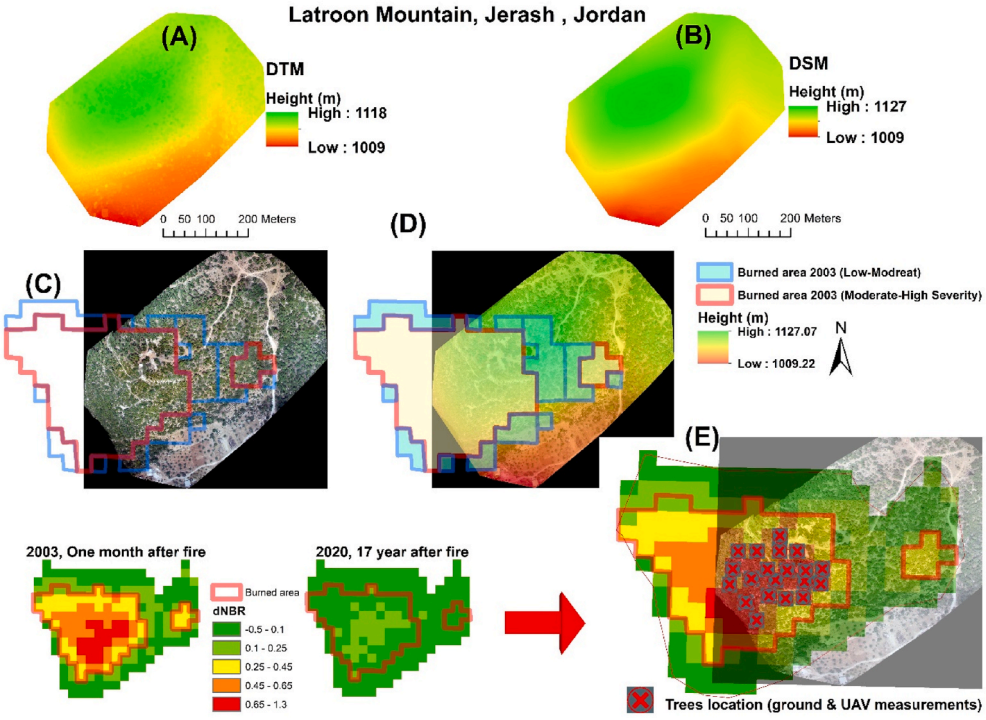

Fig. 4. (A) Digital Terrain Model (DTM), (B) Digital Surface Model (DSM) and (C) orthorectified image obtained with a UAV was overlaid with the burned area in 2003 (D) to derive tree height. (E) Landsat-dNBR image for 2003 and 2020 were overlaid to identify the best trees for ground measurements.

vegetation height captured in the DTM and DSM ranged from 0.3 m (shrubs) to 12 m (Pine trees) across the study area. Tree heights in 2020 from the area burned in 2003 were between 2 and 10 m depending on plant species and burn severity.

Plant height from ground measurements and UAV data are presented in Fig. 5. Trees from severely burned areas (Landsat-dNBR, 2003) had lower heights than those from the moderate severity class across the studied species. In both datasets tree heights in the moderate-severe class was about 35%–40% higher than high severity class for *Arbutus andrachne*, 125%–135% for *Pinus halepensis* and 100%–115% for *Quercus coccifera* (Fig. 5). Ground measurements mean were often higher (3%–9%) than the UAV estimates. However, tree height derived from UAV data and ground reference measurements were statically similar in both severity classes (moderate-severe, high severity) and across plant species, *Arbutus andrachne*, *Pinus halepensis* and *Quercus coccifera*.

Leaf and canopy temperatures from moderate and high severity Landsat-dNBR classes were similar across all three species (Fig. 6 a and b). However, *Arbutus andrachne* leaf temperature was significantly lower than *Pinus halepensis* in the moderate-severe dNBR plots (Fig. 6 c). In addition, the bare soil temperature (the average of shaded and sunny areas) was significantly higher than the leaf and canopy temperature (Fig. 6 d). Mean temperature for bare soil was 42.1 °C, leaf 34.5 °C and canopy (1 m far from tree) was 26.4 °C.

Gas exchange (*Pn*, *gs* and *E*) and chlorophyll content index from moderate and high severity plots were inconsistent or not significant across species (Fig. 7). Although the chlorophyll content of *Arbutus andrachne* in the moderate-severe class were lower than the high severity class, the same plot had higher *gs* and *E* and similar *Pn* compared to high severity plots. However, *Pn* (μmol m^{-2} s^{-1}) and chlorophyll content index were higher than 15 across plant species and in both dNBR burned classes (Fig. 7).

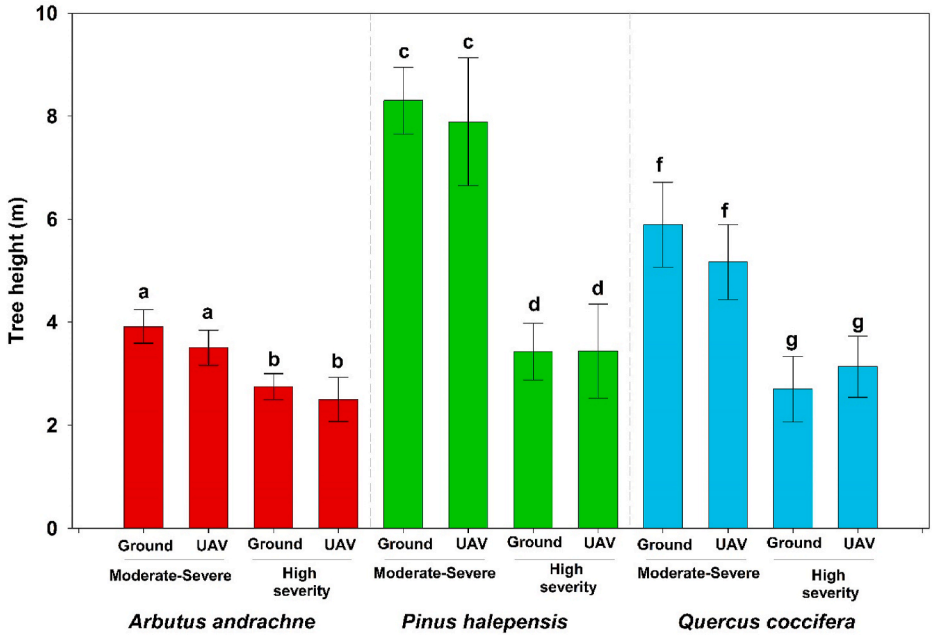

Fig. 5. Tree height of *Arbutus andrachne*, *Pinus halepensis* and *Quercus coccifera* from ground measurements and unmanned aerial vehicle (UAV) in September 2020. Moderate and high severity class plots were determined using the Landsat-dNBR image of 2003. Different letters above bars and within species indicate significant differences in tree height according to Tukey's HSD test ($P \leq 0.05$).

4. Discussion

4.1. Assessment of forest fire severity and recovery using landsat ETM + data

Wildfire is an essential mechanism for Earth ecosystems and forest regeneration (Amos et al., 2019; De Santis and Chuvieco, 2007). However, those fires can lead to massive devastation to ecosystems as well human socio-economic factors (Amos et al., 2019). In fact, forest fires have substantial impact on greenhouse gas emission and ecosystem production (Sannigrahi et al., 2020). Therefore, accurate, consistent, and timely burn severity records are necessary for planning, managing and restoration after forest fires (Amos et al., 2019). However, wildlife fires are often located in areas far from human residence and observation and in most cases the access to forest fire regions is both difficult and dangerous (Amos et al., 2019). Forest supervisors need reliable techniques to evaluate post-fire recovery and delineate management activities across the area, which might be highly expensive and resource-consuming in terms of data gathering (Fernández-Guisuraga et al., 2019). In this context, remote sensing approaches enable the collection of environmental data over a large scale with low input efforts (Fernández-Guisuraga et al., 2019; Othman et al., 2014). Remote sensing using satellite and airborne sources can provide a multi-temporal (rapid), inexpensive (free of charge, less labour), and consistent overview of vegetation (Amos et al., 2019; Othman et al., 2014, 2018). In this study, Landsat ETM + images were used to estimate fire severity and the recovery process (Table 2 and Fig. 4). Landsat sensors provide coarser spatial resolution compared to high spatial and temporal resolution sensors but may offer several advantages over those hyper spatial sensors, including wider spectrum coverage, specifically in the SWIR region (Arnett et al., 2015; Wulder et al., 2008). Tree moisture content and water potential represent the water status of the plant and their values are perquisite for remote sensing of spatial and temporal variations of live fuel moisture content (Othman et al., 2014, 2018; Yebra et al., 2013). Changes in live fuel moisture content have both direct (liquid water absorption, SWIR bands) and indirect (pigment and structural changes, NIR bands) impacts on spectral reflectance (Yebra et al., 2013). Water status in trees has a direct effect on spectral reflectance through the absorption of radiation within the NIR and SWIR spectral regions, 970, 1200, 1450, 1940, and 2500 nm (Othman et al., 2014, 2015; Yebra et al., 2013). Overall, the Landsat program provides a continuous and valuable record of vegetation (chlorophyll content, water status, cover density) for more than 50 years at no cost (Othman et al., 2021; Sawalhah et al., 2018; Wulder et al., 2008). Those forest health variables can be linked to forest fires.

Landsat-dNBR for the pre and post fire of Latroon forest showed clearly the extent and the severity of burdened area as well as the recovery process during the study period, 2003–2020. Although the ground measurements (2020) of chlorophyll and gas exchange were inconsistent across the burned area, the Landsat-dNBR images showed that the moderate and severely-burned area (2003) did not fully recovered (Fig. 3). This imply the usefulness of using Landsat-dNBR data for detect the forest fire extent and severity. The most suitable way to assess wildfire severity using Landsat sensors images is by discriminating unburned and burned pixels according to their NBR pre-/post-fire difference values, dNBR (Escuin et al., 2008). Vegetation indices such as normalized difference vegetation index (NDVI), enhanced vegetation index (EVI) normally detect immediate post fires because those indices are sensitive to the greenness of the plants (chlorophyll) but the accuracy of those indices decreases in parallel with forest recovery (Chen et al., 2011; Escuin et al., 2008). For example, after the fires in Black Hills National Forest, South Dakota, in 2000, the Landsat-NDVI, EVI and NBR of pre- and post-fire were correlated with 66 field-based composite burn index (CBI) plots for 7 years (Chen et al., 2011). The differences of NDVI and EVI between the pre-fire years was highly correlated with CBI in first two years after fire ($0.7<r<0.86$) but decreased significantly thereafter ($0.2<r<0.7$). Interestingly, the delta dNBR (deference of NBR between pre and post fire) had consistently good correlation ($0.6<r<0.82$) with CBI scores across the study period (2000–2007). Amos et al. (2019) found that the visible region of the electromagnetic spectrum from Sentinel-2A was not well suited to discriminate burned from unburned land cover but NBR produced the best results for detecting burnt areas. The dNBR proved to be the most efficient remotely sensed index for assessing burn severity in Peloponnese forests, Greece, followed by delta Normalized Difference Moisture Index (dNDMI) and delta NDVI (dNDVI) (Veraverbeke et al., 2011). The

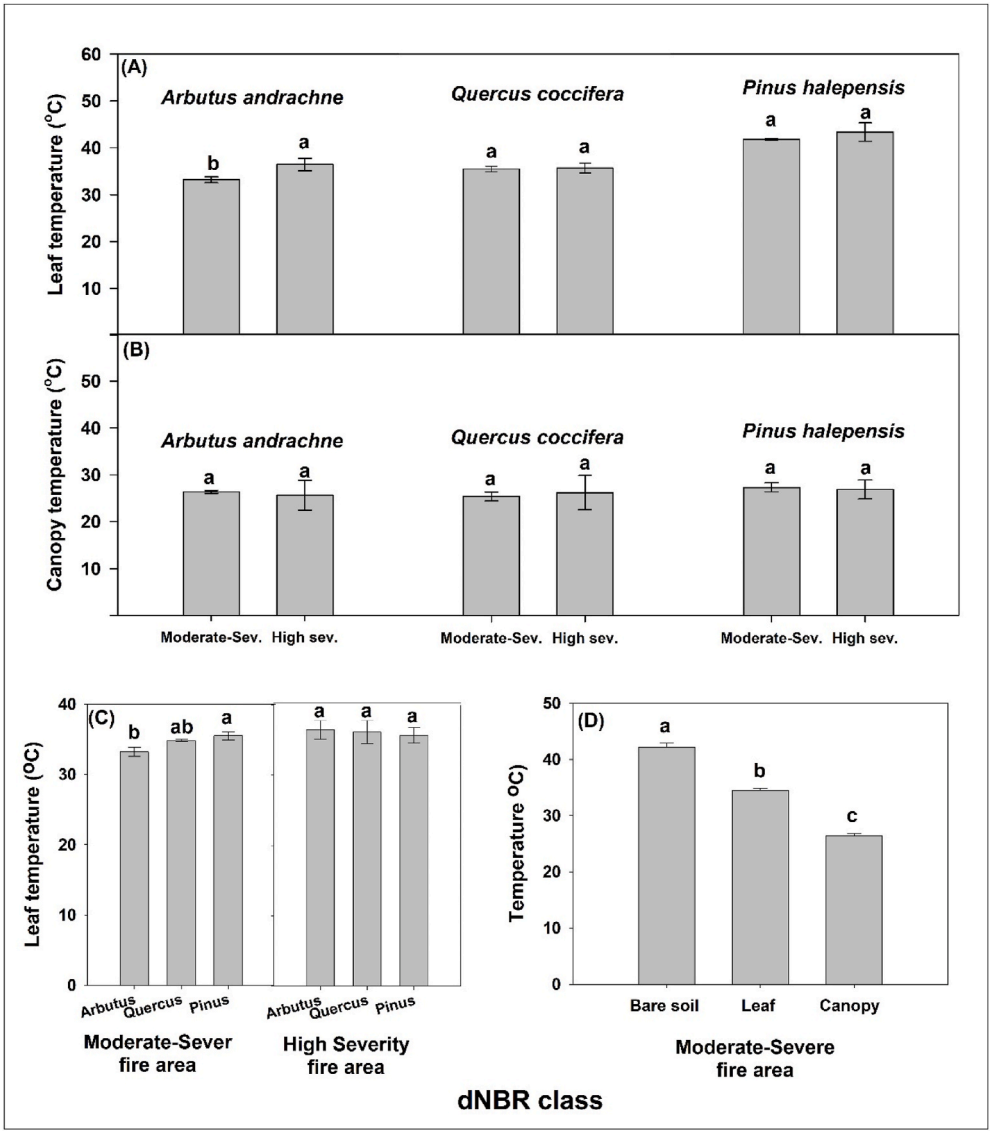

Fig. 6. Canopy, leaf temperature and bare soil (average of shady and sunny area) temperature of *Arbutus andrachne*, *Pinus halepensis* and *Quercus coccifera.* Moderate-severe and high severity plots were determine using the Landsat-dNBR image, 2003. Different letters above bars indicate significant differences in tree height according to Tukey's HSD test ($P \leq 0.05$).

coefficient of determination for between field-based Geo Composite Burn Index and dNBR was 63%, dNDMI was 48%, and dNDVI was 46% (Veraverbeke et al., 2011).

In this study, Landsat-dNBR images for pre and post fire of Lantron Mountain showed that about 65% of the forest was burned. The severity analysis of the images showed that more than 20% of the forest was extremely damaged (dNBR, 0.45–1.3). Those burned spots (moderate and highly severe burned area) required about 4 years to partially recover from that damage. In fact, after 17 year of fire, 2020, the Landsat-dNBR data showed that about 24% of the moderate and severely burned area in 2003 which estimated by 23% of the forest are not fully recovered to the same condition before fire (Table 2). The slow recovery rate could be attribute to the dry climate in Jerash, Jordan. Jarash, including Dibeen and Latroon Mountain forests is the driest part of the world in which the *Pinus halepensis* are known to grow naturally, with an average annual rainfall of about 400 mm (RSCN, 2015). Considering the slow recovery results (Landsat-dNBR) due to fragile environment, intensive legislation and management laws should be applied to protect this species (*Pinus halepensis*) in this area which represent the southeastern geographical limit of this forest type worldwide (RSCN, 2015).

4.2. Forest status using ground morphophysiology, UAV and landsat datasets

Although UAV slightly underestimated the tree height (less than 9%), UAV means were statistically similar to ground measurement data across the severity classes and over the tested species (Fig. 5). UAV measurements of tree height tended to be lower than the actual values (Kameyama and Sugiura, 2020). However, the deviation from the ground measurement is not significant (Balenović et al., 2015). Overall, our results were consistent with previous studies. While satellite sensor images are widely used for forest fire assessments, they might show some weaknesses. It may take too long to obtain imagery of the burned area because the temporal resolution is not controlled by the user, cloud cover in the imagery, and the spatial resolution could be insufficient to capture small features (Pérez-Rodríguez et al., 2020). Nowadays, only Sentinel-2 images (20 m spatial resolution) are available at good temporal resolution (5 days revisit frequency) with no charges. In this context, UAVs equipped with high spatial resolution cameras may assist

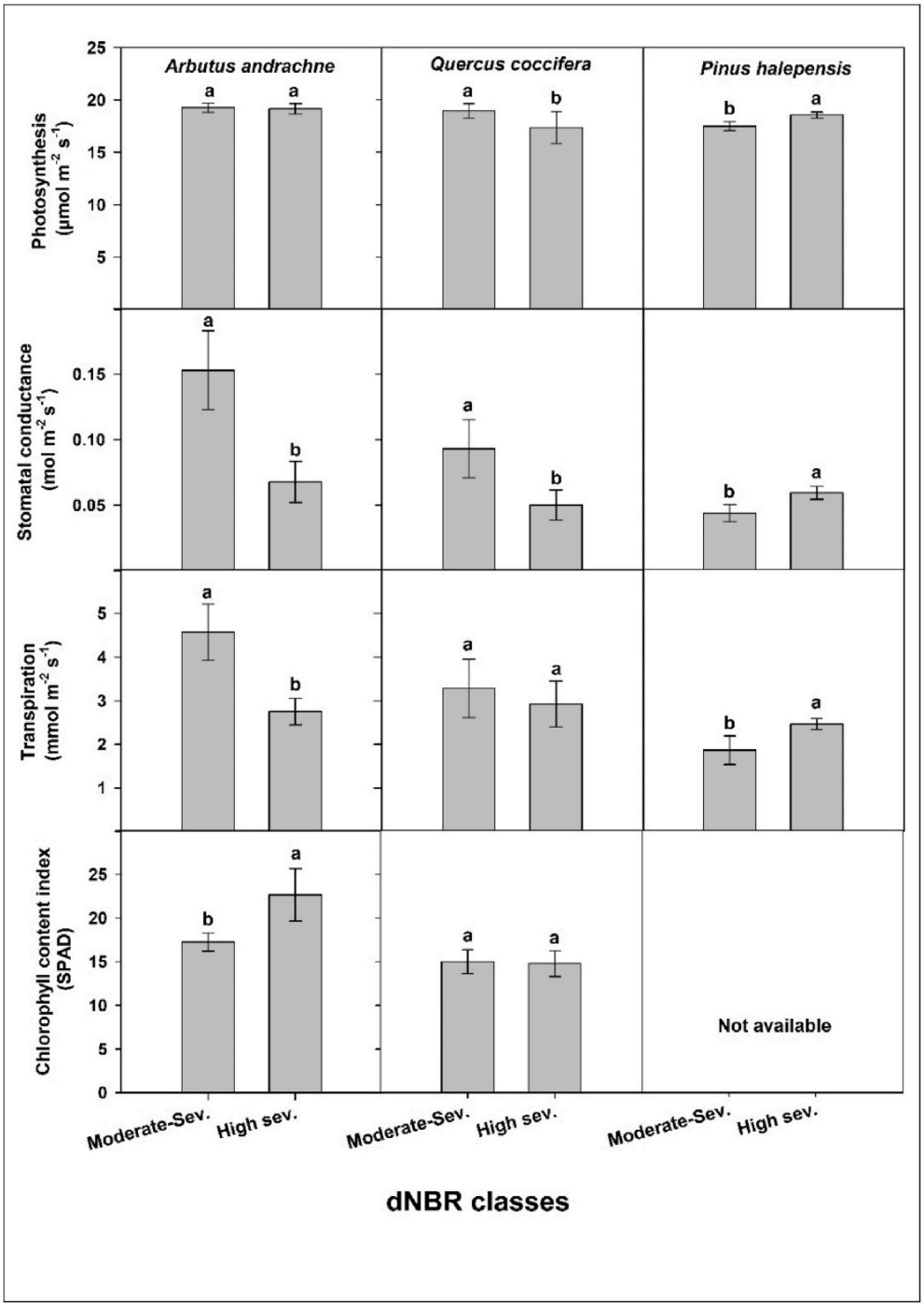

Fig. 7. Gas exchange (photosynthesis, stomatal conductance, and transpiration) and chlorophyll content index (SPAD) of *Arbutus andrachne*, *Quercus coccifera*, and *Pinus halepensis* leaves from moderate-severe and high severity plots identified using the dNBR-Landsat image one month after fire incidence (October 2003). Needle leaf shape restricted the SPAD measurements of *Pinus*. Different letters above bars indicate significant differences between treatments according to Tukey's HSD test ($P \leq 0.05$).

in these situations especially when flight timing is critical. UAVs offer higher spatial and temporal resolution and offer many opportunities to map fine scale forest attributes and examine the impact of fire on forests (Pérez-Rodríguez et al., 2020). High resolution (RGB, visible spectrum) cameras coupled with Structure from Motion and multi-view stereopsis techniques are usually used in UAV- photogrammetric projects to produce high quality DSM, DTM and mosaic orthorectified images (Carvajal-Ramírez et al., 2019; Fonstad et al., 2013; Furukawa et al., 2010). The assessment of burn severity patterns using Probabilistic Neural Networks algorithms (PNN) based on field data and (20 cm) image products derived from a UAV correctly classified 84.3% of vegetation and 77.8% of soil burn severity levels (Pérez-Rodríguez et al., 2020). However, if the post-fire day is cloudy, even UAV images are not useful as consequence of the different solar illumination conditions. Overall, UAV hold promise for identifying plant morphology, specifically the tree height.

To assess the sensitivity of Landsat-dNBR data, seven trees from three species were selected from the moderate-severe (0.45–0.6) and high severity (0.65–1.3) classes. Those trees were selected from the pixels where high severity-burned trees converted to the low severity class in 2020 in the dNBR images (Fig. 4 E). In 2020, most moderate-severe as well as high severity class areas converted to low severity class (dNBR 0.1–0.25). This mean that trees height of either the low-moderate and severe classes (Landsat-dNBR, 2003) which converted to the same class in 2020 is expected be similar. While the Landsat-dNBR image in 2020 classified those pixels (moderate or high severity, 2003) into the same

severity category, ground reference measurements and UAV data revealed that the tree height of those plots (similar class according to dNBR, 2020) was extremely different (Figs. 3 and 5). For example, *Pinus halepensis* trees from the severely-burned area in 2003 was more than 4 m shorter (deference in height 135%) than low-moderate plots according to ground and UAV results (Fig. 5). Overall, Landsat-dNBR did not detect the prolonged morphological (plant height) changes accurately after forest fire. This result is expected because Landsat sensors as other optical systems (if not in stereoscopic pair) do not allows to detect tree's height.

Changes in leaf pigment concentrations, such as chlorophyll, produce changes in visible and NIR reflectance and co-vary with live fuel moisture content (Yebra et al., 2013). In this study, the chlorophyll content index and *Pn* were inconsistent across fire severity class. However, their values were within the acceptable levels across fire severity and species. Although canopy temperature was similar across dNBR classes, *Arbutus andrachne* had lower leaf temperature than *Pinus halepensis.* Higher leaf temperatures in *Pinus halepensis* than *Arbutus andrachne* could partially explain the high flammability behavior of pine trees compared to other species. In addition, bare soil temperature was 59.5% higher than canopy temperature. This result highlight the important of vegetation cover in mitigating the weather conditions, specifically temperature.

Time series remote sensing indices for post-fire studies are sometimes unrealistic and biased due to the saturation issues of vegetation indices which lead to an underestimation of the forest successional stages and an overestimation of the forest recovery rate (Chu et al., 2016). In addition, the use moderate spatial resolution sensors such as Landsat (30 m) to delineate small details in the burned areas could be controversial. For example, in our study, the recovery assessment of the forest fire across the study period 2003–2020 required detailed information about the canopy diameter and height. Those data are available using Landsat sensor images. The assessment of burn severity across Mediterranean forest in Vesuvius National Park, Italy using medium-spatial resolution satellite imagery (Landsat-8 and Sentinel-2A) and field data revealed a very low agreement ($0.15 < K < 0.21$) between the burn severity class obtained from field-based indices (Composite Burn Index (CBI) and its geometrically modified version CBI) and dNBR derived from satellite sensor data (Saulino et al., 2020). Therefore, coupling medium-spatial resolution satellite imagery and field-based data is necessary to detect burn severity across Mediterranean forests. Coarse special resolution images from satellite sensors could lower the accuracy results especially small burdened areas. Arnett et al. (2015) assessed the usefulness of using the RapidEye (5 m) constellation and Landsat (Thematic Mapper TM, and Operational Land Imager OLI (30 m) for detection small low severity fires in Western Canadian forest. EVI, NBR, and Soil Adjusted Vegetation Index (SAVI) derived from both sources were correlated with field reference data (simple burn index). Although all correlations between the ground and satellite sensors indices were significant ($p < 0.01$), overall accuracy was substantially varied across sensors. The RapidEye provided much more spatially detailed estimates of tree damage. Compared to Landsat (30 m), the high spatial resolution sensor (RapidEye, 5 m) had the potential to map fine scale forest attributes and resolve fire damage at the individual tree level. However, RapidEye does not have spectral information in the SWIR (water bands). This is important because the shortwave spectrum provides substantial information about water status in trees (Othman et al., 2014, 2015). Tree water status pre- and post-fire link to forest health and canopy temperature. It is therefore essential to understand the causes of fires as well as the regeneration process. Worldwide, Landsat and Sentinel images are the only free of charges, moderate temporal and spatial sensors that cover the SWIR spectral region.

5. Conclusions and policy implications

Overall, forest fires in Jordan have a long-lasting negative impact. Due to the climatic conditions, the recovery process can prolong to decades. In this study, Landsat-dNBR images revealed that the Latroon forest experienced a severe forest in August 2003 which lead to potential damage of 62% of the forest. Although recent Landsat-dNBR image (2020) classified moderate and high severity burned area that occurred in 2003 into the same severity category, ground reference measurements and UAV data revealed that the tree height of those plots (similar class according to dNBR, 2020) was extremely different, especially for *Pinus halepensis*; trees from the severely-burned area in 2003 were 135% shorter than the low-moderate plots according to ground and UAV results. Overall, Landsat-dNBR did not detect the prolonged morphological (plant height) changes accurately after forest fire. Remote sensing from Landsat ETM + coupled with ground measurements and UAV data has the potential to improve our forest fire assessment by mapping fine scale forest attributes and examining the physiology of trees such as chlorophyll content and plant water status. While UAV can potentially estimate the tree height, surface reflectance data from Landsat sensors (NIR, vegetation greenness and density, SWIR, water status) hold promise for estimating the physiology of the canopy.

Trends and projections of climate change in Jordan require new interventions and policies to mitigate and adapt to the causative factors for forest fires. More specifically, to: (1) control the development in the fire-prone ecosystems (reducing hazards from buildings and utilizing forests) and introduce the participatory management option to suppress incidences, as people must be prepared for taking actions for controlling the early phase of fires, (2) establish an inventory of forest types and status according to historically high frequency, and low-to moderate-severity fire regimes, and the assessment of forests survived of past high-fire periods for mapping potential fire locations for different types of forests, (3) set-up financial mechanisms for alleviating forest fires through preparing and executing efficient forest management plans that involve comprehensive rehabilitation and restorations activities.

Credit author statement

Bassam Qarallah: Writing – original draft, Investigation, Data curation, Visualization, Malik Al-Ajlouni: Methodology, Investigation, Data curation, Ayman Al-Awasi: Methodology, Investigation, Data curation, Mohammad AlKarmy: Methodology, Investigation, Data curation, Emad Al-Qudah: Methodology, Investigation, Data curation, Ahmad Bani Naser: Methodology, Investigation, Data curation, Amani Al-Assaf: Writing – review & editing, Caroline M. Gevaert: Writing – review & editing, Yolla Al Asmar: Writing – review & editing, Mariana Belgiu: Writing – review & editing, Yahia A. Othman: Formal analysis, Writing – review & editing, Writing – original draft.

Declaration of competing interest

The authors declare that they have no known competing financial interests or personal relationships that could have appeared to influence the work reported in this paper.

Acknowledgments

We thank Netherlands UniversitiesFoundation for International Cooperation (Nuffic), Royal Department for Environment Protection (RANGERS) for their support.

References

Al-Assaf, A., Al-Asmar, Y., Johnsen-Harris, B., Al-Raggad, M., 2016. Spatial mapping of the social value of forest services: a case study of northern Jordan. J. Sustain. For. 35, 469–485. https://doi.org/10.1080/10549811.2016.1212381.

Al-assaf, A., Nawash, O., Omari, M., 2014. Identifying forest ecosystem services through socio-ecological bundles: a case study from northern Jordan. Int. J. Sustain. Dev. World Ecol. 21, 314–321. https://doi.org/10.1080/13504509.2014.919968.

Al-Eisawi, A., 2012. Conservation of natural ecosystems in Jordan. Pakistan J. Bot. 44, 95–99.
Alkhatib, A.A., 2014. A review on forest fire detection techniques. Int. J. Distributed Sens. Netw. 10, 597368.
Amos, C., Petropoulos, G., Ferentinos, K., 2019. Determining the use of Sentinel-2A MSI for wildfire burning & severity detection. Int. J. Rem. Sens. 40 (3), 905–930. https://doi.org/10.1080/01431161.2018.1519284.
Arnett, J., Coops, N., Daniels, L., Falls, R., 2015. Detecting forest damage after a low-severity fire using remote sensing at multiple scales. Int. J. Appl. Earth Obs. Geoinf. 35, 239–246.
Balenović, I., Seletković, A., Pernar, R., Jazbec, A., 2015. Estimation of the mean tree height of forest stands by photogrammetric measurement using digital aerial images of high spatial resolution. Ann. For. Res. 58, 125–143.
Cansler, C.A., McKenzie, D., 2014. Climate, fire size and biophysical setting control fire severity and spatial pattern in the northern Cascade Range, USA. Ecol. Appl. 24, 1037–1056.
Carvajal-Ramírez, F., Marques, D., Agüera-Vega, F., Martínez-Carricondo, P., Serrano, J., Moral, F., 2019. Evaluation of fire severity indices based on pre- and post-fire multispectral imagery sensed from UAV. Rem. Sens. 11, 993. https://doi.org/10.3390/rs11090993.
Chen, X., Vogelmann, J., Rollins, M., Ohlen, D., Key, C., Yang, L., Huang, C., Shi, H., 2011. Detecting post-fire burn severity and vegetation recovery using multitemporal remote sensing spectral indices and field-collected composite burn index data in a ponderosa pine forest. Int. J. Rem. Sens. 32, 7905–7927. https://doi.org/10.1080/01431161.2010.524678.
Chu, T., Guo, X., Takeda, K., 2016. Remote sensing approach to detect post-fire vegetation regrowth in Siberian boreal larch forest. Ecol. Indicat. 62, 32–46. https://doi.org/10.1016/j.ecolind.2015.11.026.
Chuvieco, E., Martín, M., Palacios, A., 2002. Assessment of different spectral indices in the red-near-infrared spectral domain for burned land discrimination. Int. J. Rem. Sens. 23, 5103–5110. https://doi.org/10.1080/01431160210153129.
De Santis, A., Chuvieco, E., 2007. Burn severity estimation from remotely sensed data: performance of simulation versus empirical models. Remote Sens. Environ. 108, 422–435. https://doi.org/10.1016/j.rse.2006.11.022.
Escuin, S., Navarro, R., Fernández, P., 2008. Fire severity assessment by using NBR (normalized burn ratio) and NDVI (normalized difference vegetation index) derived from LANDSAT TM/ETM images. Int. J. Rem. Sens. 29, 1053–1073. https://doi.org/10.1080/01431160701281072.
Fernández-Guisuraga, J., Calvo, L., Fernández-García, V., Marcos-Porras, E., Taboada, A., Suárez-Seoane, S., 2019. Efficiency of remote sensing tools for post-fire management along a climatic gradient. For. Ecol. Manag. 433, 553–562. https://doi.org/10.1016/j.foreco.2018.11.045.
Filipponi, F., 2019. Exploitation of Sentinel-2 time series to map burned areas at the national level: a case study on the 2017 Italy wildfires. Rem. Sens. 11, 622. https://doi.org/10.3390/rs11060622.
Flannigan, M., Krawchuk, M., de Groot, W., Wotton, B., Gowman, L., 2009. Implications of changing climate for global wildland fire. Int. J. Wildland Fire 18, 483–507.
French, N., Kasischke, E., Hall, R., Murphy, K., Verbyla, D., Hoy, E., Allen, J., 2008. Using Landsat data to assess fire and burn severity in the North American boreal forest region: an overview and summary of results. Int. J. Wildland Fire 17, 443–462.
Fonstad, M., Dietrich, J., Courville, B., Jensen, J., Carbonneau, P., 2013. Topographic structure from motion: a new development in photogrammetric measurement. Earth Surf. Process. Landforms 38, 421–430.
Furukawa, Y., Ponce, J., 2010. Accurate, dense, and robust multiview stereopsis. IEEE Trans. Pattern Anal. Mach. Intell. 32, 1362–1376.
Gao, B.C., 1996. NDWI – a normalized difference water index for remote sensing of vegetation liquid water from space. Remote Sens. Environ. 58, 257–266.
Gibson, R., Danaher, T., Hehir, W., Collins, L., 2020. A remote sensing approach to mapping fire severity in south-eastern Australia using sentinel 2 and random forest. Remote Sens. Environ. 240, 111702. https://doi.org/10.1016/j.rse.2020.111702.
Hammill, K., Bradstock, R., 2006. Remote sensing of fire severity in the Blue Mountains: influence of vegetation type and inferring fire intensity. Int. J. Wildland Fire 15, 213–226.
Huete, A., Didan, K., Miura, T., Rodriguez, E., Gao, X., Ferreira, L., 2002. Overview of the radiometric and biophysical performance of the MODIS vegetation indices. Remote Sens. Environ. 83, 195–213.
Kameyama, S., Sugiura, K., 2020. Estimating tree height and volume using unmanned aerial vehicle photography and SfM technology, with verification of result accuracy. Drones 4, 19. https://doi.org/10.3390/drones4020019.
Keeley, J., Syphard, A., 2016. Climate change and future fire regimes: examples from California. Geosciences 6, 37. https://doi.org/10.3390/geosciences6030037.
Langenfelds, R., Francey, R., Pak, B., Steele, L., Lloyd, J., Trudinger, C., Allison, C., 2002. Interannual growth rate variations of atmospheric CO2 and its $\delta^{13}C$, H_2, CH_4 and CO between 1992 and 1999 linked to biomass burning. Global Biogeochem. Cycles 16 (3), 1048. https://doi.org/10.1029/2001GB001466, 2002.
Leskovar, D., Othman, Y., 2021. Direct seeding and transplanting influence root dynamics, morpho-physiology, yield, and head quality of globe artichoke. Plants 10 (5), 899. https://doi.org/10.3390/plants10050899.
Othman, Y., Al-Ajlouni, M., St Hilaire, R., 2019. Using hyperspectral surface reflectance data to detect chlorophyll content in pecans. Fresenius Environ. Bull. 28, 6117–6124.
Othman, Y., Steele, C., Van Leeuwen, D., Heerema, R., Bawazir, S., Hilaire, R., 2014. Remote sensing used to detect moisture status of pecan orchards grown in a desert environment. St. Int. J. Rem. Sens. 35 (3), 949–966.
Othman, Y., Steele, C., St Hilaire, R., 2018. Surface Reflectance Climate Data Records (CDRs) is a reliable Landsat ETM+ source to study chlorophyll content in pecan orchards. Journal of the Indian Society of Remote Sensing 46 (2), 211–218.
Othman, Y., St Hilaire, R., 2021. Using multispectral data from Landsat ETM+ to estimate leaf area index of pecan orchards. Fresenius Environ. Bull. 30, 2613–2618.
Othman, Y., Steele, C., Van Leeuwen, D., St Hilaire, R., 2015. Hyperspectral surface reflectance data used to detect moisture status of pecan orchards during flood irrigation. J. Am. Soc. Hortic. Sci. 140, 449–458.
Pérez-Rodríguez, L., Quintano, C., Marcos, E., Suarez-Seoane, S., Calvo, L., Fernández-Manso, A., 2020. Evaluation of prescribed fires from Unmanned Aerial Vehicles (UAVs) imagery and machine learning algorithms. Rem. Sens. 12 (8), 1295. https://doi.org/10.3390/rs12081295.
Quintano, C., Fernandez-Manso, A., Marcos, E., Calvo, L., 2019. Burn severity and post-fire land surface albedo relationship in Mediterranean forest ecosystems. Rem. Sens. 11, 2309. https://doi.org/10.3390/rs11192309.
RSCN, 2015. Dibeen forest reserve. Royal society for the conservation of nature. Accessed March, 2021. https://www.rscn.org.jo/content/dibeen-forest-reserve-0.
Sannigrahi, S., Pilla, F., Basu, B., Basu, A., Sarkar, K., Chakraborti, S., Joshi, P., Zhang, Q., Wang, Y., Bhatt, S., Bhatt, A., Jha, S., Keesstra, S., Roy, P., 2020. Examining the effects of forest fire on terrestrial carbon emission and ecosystem production in India using remote sensing approaches. Sci. Total Environ. 725, 138331. https://doi.org/10.1016/j.scitotenv.2020.138331.
Saulino, L., Rita, A., Migliozzi, A., Maffei, C., Allevato, E., Garonna, A., Saracino, A., 2020. Detecting burn severity across Mediterranean forest types by coupling medium-spatial resolution satellite imagery and field data. Rem. Sens. 12 (4), 741. https://doi.org/10.3390/rs12040741.
Sawalhah, M., Al-Kofahi, S., Othman, Y., Cibils, A., 2018. Assessing rangeland cover conversion in Jordan after the Arab spring using a remote sensing approach. J. Arid Environ. 157, 97–102.
Shishany, S., Al-Assaf, A., Majdalawi, M., Tabieh, M., Tadros, M., 2020. Factors influencing local communities relational values to forest protected areas in Jordan. J. Sustain. For. https://doi.org/10.1080/10549811.2020.1847665.
Tadros, M., Al-Assaf, A., Othman, Y., Makhamreh, Z., Taifoure, H., 2020. Evaluating the effect of *Prosopis juliflora*, an alien invasive species, on land cover change using remote sensing approach. Sustainability 12 (15), 5887. https://doi.org/10.3390/su12155887.
UNOOSA, 2021. Normalized burn ratio (NBR). The united nations office for outer space affairs. Accessed April, 2021. https://un-spider.org/advisory-support/recommended-practices/recommended-practice-burn-severity/in-detail/normalized-burn-ratio#:~:text=The%20Normalized%20Burn%20Ratio%20(NBR,shortwave%20infrared%20(SWIR)%20wavelengths.
Van Der Werf, G., Randerson, J., Giglio, L., Collatz, G., Mu, M., Kasibhatla, P., Morton, D., Defries, R., Jin, Y., Van Leeuwen, T., 2010. Global fire emissions and the contribution of deforestation, savanna, forest, agricultural, and peat fires (1997–2009). Atmos. Chem. Phys. 10, 11707–11735.
Veraverbeke, S., Lhermitte, S., Verstraeten, W., Goossens, R., 2011. Evaluation of pre/post-fire differenced spectral indices for assessing burn severity in a Mediterranean environment with Landsat Thematic Mapper. Int. J. Rem. Sens. 32, 3521–3537. https://doi.org/10.1080/01431161003752430.
Wei, X., Wang, G., Chen, T., Hagan, D., Ullah, W., 2020. A spatio-temporal analysis of active fires over China during 2003–2016. Rem. Sens. 12, 1787. https://doi.org/10.3390/rs12111787.
Wulder, M., White, J., Goward, S., Masek, J., Irons, J., Herold, M., Wood-cock, C., 2008. Landsat continuity: issues and opportunities for land cover monitoring. Remote Sens. Environ. 112 (3), 955–969.
Yebra, M., Dennison, P., Chuvieco, E., Riaño, D., Zylstra, P., Hunt, E., Danson, F., Qi, Y., Jurdao, S., 2013. A global review of remote sensing of live fuel moisture content for fire danger assessment: moving towards operational products. Remote Sens. Environ. 136, 455–468.